

Finite-Alphabet based Channel Estimation for OFDM and related Multi-Carrier Systems

Shengli Zhou and Georgios B. Giannakis¹

Dept. of ECE, Univ. of Minnesota

200 Union Street SE, Minneapolis, MN 55455

Emails: {szhou, georgios}@ece.umn.edu

Abstract — Novel blind channel estimators based on the finite alphabet property of information symbols are derived in this paper for OFDM systems. The resulting algorithms are applicable not only to standard OFDM transmitters with cyclic prefix, but also to the recently proposed zero padded OFDM transmissions. Based on FFT-processed received data, channel identifiability is guaranteed regardless of channel zero locations and various channel estimation algorithms become available by trading off complexity with performance. Unlike existing blind channel estimators, the inherent scalar ambiguity is reduced to finite phase values and is thus easily resolved. With PSK transmissions, channel estimation becomes possible even from a single OFDM symbol at high SNR. The algorithms are tested with simulations and also compared with existing alternatives in a realistic HIPERLAN/2 setting.

I. INTRODUCTION

Holding great promise for high rate transmissions, Orthogonal Frequency Division Multiplexing (OFDM) is currently being adopted and tested for many standards, including digital audio and video broadcasting (DAB, DVB) in Europe and high speed DSL modems over twisted pairs in the US. OFDM has also been proposed for local area mobile wireless broadband standards including IEEE802.11a, MMAC and HIPERLAN/2 [7].

In order to avoid Inter Symbol Interference (ISI) arising due to channel memory, conventional OFDM systems first take the inverse Fourier transform (IFFT) of data symbols and then insert redundancy in the form of a Cyclic Prefix (CP) of length larger than the FIR channel order [1]. CP is discarded at the receiver and the remaining part of the OFDM symbol is FFT processed. Combination of IFFT and CP at the transmitter with the FFT at the receiver converts the frequency-selective channel to separate flat-fading subchannels (see e.g., [1]). Frequency-domain channel equalization is then applied by dividing the FFT output by the corresponding channel frequency response. However, symbol recovery is not assured if the channel has nulls on (or close to) some subcarriers. Recently, trailing zeros (TZ) are proposed in [6] to replace the CP, in order to guarantee symbol recovery regardless of channel zeros at the cost of modifying the transmitter and complicating the equalizer.

Because they save bandwidth and are capable of coping with channel variations, blind channel estimation and equalization methods are well motivated since they avoid the use of training sequences. Numerous blind channel estimators have been

developed based on cyclostationarity [4], or subspace decompositions that exploit the TZ and the CP structure in OFDM transmissions [6],[5].

In this paper, we develop a new channel estimation method that is applicable to both CP- and TZ-OFDM transmissions and relies on the finite alphabet property of information-bearing symbols. Unlike subspace methods developed for CP-OFDM, channel identifiability is guaranteed here even when the channel has nulls on subcarriers. Moreover, subspace based methods for both CP- and TZ-OFDM require collection of long enough data records to render the data covariance matrix full rank [5],[6]. In contrast, PSK transmissions with the novel method enable channel estimation even from a single OFDM symbol at high SNR. Reducing the size of required samples equips the proposed method with the ability to track even fast channel variations. Inherent to all blind channel estimation methods is a scalar ambiguity. However, by exploiting the finite alphabet property the scalar ambiguity in our algorithms is restricted to a few phase values and is thus easily resolved.

The rest of this paper is organized as follows: Section II develops a unifying OFDM matrix model that incorporates neatly both CP and TZ variants. Section III presents the new channel estimation methods. Simulations and comparisons are presented in Section IV and conclusions are drawn in Section V.

II. MATRIX FORMULATION OF CP- AND TZ-OFDM

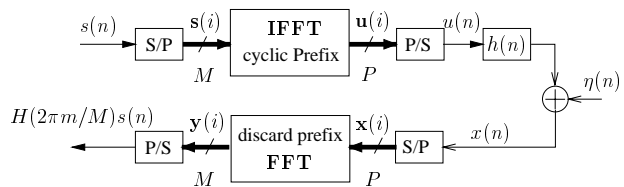


Figure 1: Conventional CP-OFDM system

The block diagram in Fig. 1 describes the conventional CP-OFDM system. First, the information stream $s(n)$ is parsed into M -long blocks: $\mathbf{s}(i) := [s(iM), s(iM+1), \dots, s(iM+M-1)]^T$, where the block index $i := \lfloor n/M \rfloor$, and $\lfloor \cdot \rfloor$ denotes the integer-floor. The $M \times 1$ symbol block $\mathbf{s}(i)$ is then mapped to a $P \times 1$ vector $\mathbf{u}(i) := [u(iP), u(iP+1), \dots, u(iP+P-1)]^T$ by taking the IFFT of $\mathbf{s}(i)$ and replicating the last $P-M$ elements in the front to form the CP.

Let \mathbf{I}_{cp} denote the last $P-M$ rows of the $M \times M$ identity matrix \mathbf{I}_M and \mathbf{F}_M be the $M \times M$ FFT matrix with (m, n) entry $(1/\sqrt{M}) \exp(-j2\pi mn/M)$. We describe the CP insertion using the $P \times M$ transmit-matrix $\mathbf{T}_{cp} := [\mathbf{I}_{cp}^T, \mathbf{I}_M^T]^T$. Matrix \mathbf{T}_{cp} along with the IFFT matrix \mathbf{F}_M^H allow us to express the i th transmitted block as: $\mathbf{u}(i) = \mathbf{T}_{cp} \mathbf{F}_M^H \mathbf{s}(i)$, where H denotes Hermitian transpose.

¹This work was supported by NSF Wireless Initiative grant no. 99-79443 and ARL grant no. DAAL01-98-Q-0648

Let $h(l), l \in [0, L]$ be the equivalent discrete time L th order FIR channel impulse response. The received signal sampled at the chip rate can then be written as:

$$x(n) = h(n) \star u(n) + \eta(n) = \sum_{l=0}^L h(l)u(n-l) + \eta(n), \quad (1)$$

where $\eta(n) = \eta(t)|_{t=nT_c}$ is filtered Additive Gaussian Noise (AGN). To avoid ISI, we assume that the CP length is larger than the channel order and state it formally as:

a0) $P - M \geq L$.

To cast (1) from a serial to a convenient matrix-vector form, we define the $P \times 1$ vectors: $\mathbf{x}(i) := [x(i), x(iP+1), \dots, x(iP+P-1)]^T$, $\boldsymbol{\eta}(i) := [\eta(iP), \eta(iP+1), \dots, \eta(iP+P-1)]^T$, and the Toeplitz channel matrices $\mathbf{H}_0, \mathbf{H}_1$ with first column $[h(0), \dots, h(L)]^T$, first row $[h(0), \dots, 0]$ for \mathbf{H}_0 ; and first column $\mathbf{0}_{P \times 1}$, first row $[0, \dots, h(L), \dots, h(1)]$ for \mathbf{H}_1 , respectively.

Relying on a0) and the fact that $h(l) = 0, \forall l \notin [0, L]$, we can write (1) as:

$$\mathbf{x}(i) = \mathbf{H}_0 \mathbf{u}(i) + \mathbf{H}_1 \mathbf{u}(i-1) + \boldsymbol{\eta}(i), \quad (2)$$

where the second term denotes Inter Block (and thus inter-OFDM-symbol) Interference (IBI).

At the receiver, the CP of length $P - M$ is removed first and FFT is performed on the remaining $M \times 1$ vector. In matrix form, this is accomplished with the receive-matrix $\mathbf{R}_{cp} := [\mathbf{0}_{M \times (P-M)}, \mathbf{I}_M]$ which removes the first $P - M$ entries from a $P \times 1$ vector. According to a0), $\mathbf{R}_{cp} \mathbf{H}_1 = \mathbf{0}$ removes IBI (and thus ISI) among OFDM symbols to obtain:

$$\begin{aligned} \mathbf{y}_{cp}(i) &= \mathbf{F}_M \mathbf{R}_{cp} \mathbf{x}(i) = \mathbf{F}_M \mathbf{R}_{cp} \mathbf{H}_0 \mathbf{u}(i) + \mathbf{F}_M \mathbf{R}_{cp} \boldsymbol{\eta}(i) \\ &= \mathbf{F}_M \mathbf{R}_{cp} \mathbf{H}_0 \mathbf{T}_{cp} \mathbf{F}_M^H \mathbf{s}(i) + \tilde{\boldsymbol{\eta}}_{cp}(i) \\ &= \mathbf{F}_M \tilde{\mathbf{H}} \mathbf{F}_M^H \mathbf{s}(i) + \tilde{\boldsymbol{\eta}}_{cp}(i), \end{aligned} \quad (3)$$

where $\tilde{\boldsymbol{\eta}}_{cp}(i) := \mathbf{F}_M \mathbf{R}_{cp} \boldsymbol{\eta}(i)$ is the filtered noise vector and $\tilde{\mathbf{H}} = \mathbf{R}_{cp} \mathbf{H}_0 \mathbf{T}_{cp}$ is the resulting channel matrix. It can be easily verified that $\tilde{\mathbf{H}}$ is an $M \times M$ circulant matrix with its (k, l) th entry given by $h((k-l) \bmod M)$. Because $\tilde{\mathbf{H}}$ is a circulant matrix, it is well known that $\mathbf{F}_M \tilde{\mathbf{H}} \mathbf{F}_M^H$ is a diagonal matrix $\mathbf{D}(H) := \text{diag}(H(0), H(\exp(j2\pi/M)), \dots, H(\exp(j2\pi(M-1)/M)))$, where the diagonal elements are values of the channel frequency response $H(z) = \sum_{l=0}^L h(l)z^{-l}$ evaluated at the sub-carriers $z = \exp(j2\pi m/M)$, $m = 0, 1, \dots, M-1$ (see e.g., [3, p. 202] for a proof). Therefore, we can rewrite (3) as:

$$\mathbf{y}_{cp}(i) = \mathbf{D}(H) \mathbf{s}(i) + \tilde{\boldsymbol{\eta}}_{cp}(i). \quad (4)$$

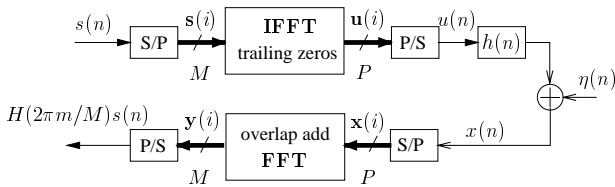


Figure 2: TZ-OFDM system

An alternative approach to removing IBI is to add trailing zeros (TZ) instead of the CP, as shown in Fig. 2 (see also [6]). To implement TZ at the transmitter, the mapping matrix \mathbf{T}_{cp} must be replaced by: $\mathbf{T}_{tz} := [\mathbf{I}_M^T, \mathbf{0}_{M \times (P-M)}^T]^T$. Note that IBI is canceled now at the transmitter because $\mathbf{H}_1 \mathbf{T}_{tz} = \mathbf{0}$. Therefore, $\mathbf{u}(i) = \mathbf{T}_{tz} \mathbf{F}_M^H \mathbf{s}(i)$, and

$$\mathbf{x}(i) = \mathbf{H}_0 \mathbf{u}(i) + \mathbf{H}_1 \mathbf{u}(i-1) + \boldsymbol{\eta}(i) = \mathbf{H}_0 \mathbf{T}_{tz} \mathbf{F}_M^H \mathbf{s}(i) + \boldsymbol{\eta}(i). \quad (5)$$

Because matrix $\mathbf{H}_0 \mathbf{T}_{tz} \mathbf{F}_M^H$ is full rank, time domain Zero-Forcing (ZF) equalization can be applied to recover the transmitted data as detailed in [6]. Furthermore, TZ-OFDM can also adopt an FFT-based low complexity receiver. Indeed, if we let \mathbf{I}_{tz} denote the first $P - M$ columns of \mathbf{I}_M , the matrix $\mathbf{R}_{tz} := [\mathbf{I}_M, \mathbf{I}_{tz}]$ maps a $P \times 1$ vector to an $M \times 1$ vector by adding the last $P - M$ elements to its first $P - M$ elements. After performing FFT on $\mathbf{R}_{tz} \mathbf{x}(i)$, we obtain:

$$\mathbf{y}_{tz}(i) = \mathbf{F}_M \mathbf{R}_{tz} \mathbf{x}(i) = \mathbf{F}_M \mathbf{R}_{tz} \mathbf{H}_0 \mathbf{T}_{tz} \mathbf{F}_M^H \mathbf{s}(i) + \mathbf{F}_M \mathbf{R}_{tz} \boldsymbol{\eta}(i). \quad (6)$$

Defining $\tilde{\boldsymbol{\eta}}_{tz}(i) := \mathbf{F}_M \mathbf{R}_{tz} \boldsymbol{\eta}(i)$ and verifying that $\mathbf{R}_{tz} \mathbf{H}_0 \mathbf{T}_{tz} = [\mathbf{I}_M, \mathbf{I}_{tz}] \mathbf{H}_0 [\mathbf{I}_M^T, \mathbf{0}^T]^T = \tilde{\mathbf{H}}$ allow us to re-write (6) as:

$$\mathbf{y}_{tz}(i) = \mathbf{F}_M \tilde{\mathbf{H}} \mathbf{F}_M^H \mathbf{s}(i) + \tilde{\boldsymbol{\eta}}_{tz}(i) = \mathbf{D}(H) \mathbf{s}(i) + \tilde{\boldsymbol{\eta}}_{tz}(i). \quad (7)$$

Equations (4) and (7) reveal that CP-OFDM and TZ-OFDM yield the same equivalent channel model and both convert the FIR convolutive channel to parallel flat fading subchannels. Through the transmit-receive mappers ($\mathbf{T}_{cp}, \mathbf{R}_{cp}$) and ($\mathbf{T}_{tz}, \mathbf{R}_{tz}$) introduced herein, it is transparent that both approaches turn linear convolution into circular convolution that can be efficiently implemented via FFTs.

Unlike subspace-based channel estimation methods [6, 5] that utilize structure information of the *pre*-FFT-processed data $\mathbf{x}(i)$, our channel estimation methods will rely on *post*-FFT-processed data $\mathbf{y}_{cp}(i)$ of (4) or $\mathbf{y}_{tz}(i)$ of (7), which will be henceforth adopted for both CP-OFDM and TZ-OFDM. Therefore, we subsequently drop the subscripts *cp/tz* and express (4) and (7) in scalar form as:

$$y(i; m) = H(\rho_m) s(i; m) + \tilde{\eta}(i; m), \quad m \in [0, M-1], \quad (8)$$

where we assign a double argument $(i; m)$ to quantities with argument $n = iM + m$ and introduce $\{\rho_m := \exp(j2\pi m/M)\}_{m=0}^{M-1}$ for notational brevity.

III. BLIND CHANNEL ESTIMATION

We will start with channel identifiability issues from the noiseless version of (8): $y(i; m) = H(\rho_m) s(i; m)$, where we omitted noise since we are concerned with basic feasibility questions first. Henceforth, we will also assume that:

- a1a)** Symbols are drawn from a finite alphabet set of size Q ; i.e., $s(i; m) \in \{\zeta_q\}_{q=1}^Q$;
- a1b)** Symbols are equiprobable ($\Pr(s(i; m) = \zeta_q) = 1/Q, \forall q$);
- a2)** Noise $\tilde{\eta}(i; m)$ is zero-mean complex circular Gaussian and independent of $s(i; m)$.

Assumption a1a) implies the following equation: $\prod_{q=1}^Q [s(i; m) - \zeta_q] = 0$. Expanding the product yields a Q th-order polynomial in $s(i; m)$: $s^Q(i; m) + \alpha_1 s^{Q-1}(i; m) + \dots + \alpha_Q = 0$, where $\alpha_1, \dots, \alpha_Q$ are determined by the constellation $\{\zeta_q\}_{q=1}^Q$ and can not all be zero. Let J be the smallest index of nonzero elements in the coefficient set $\{\alpha_j\}_{j=1}^Q$, i.e.,

Definition 1: We define J such that $\alpha_J \neq 0; \alpha_n = 0, \forall n < J$.

We can easily verify that $J = 2$ for BPSK, while $J = 4$ for QPSK and QAMs. The facts that $J \leq Q$ and that for large signal constellations $J \ll Q$, will play a key role in the rest of our paper.

Under a1b), we prove in [8] that $E\{s^J(i; m)\} = -(J/Q)\alpha_J \neq 0$. Hence, starting from $E\{y^J(i; m)\} = H^J(\rho_m) E\{s^J(i; m)\}$, we deduce that:

$$H^J(\rho_m) = \frac{-Q}{J\alpha_J} E\{y^J(i; m)\}, \quad \forall m \in [0, M-1]. \quad (9)$$

To express $H^J(\rho_m)$ in terms of $h(n)$, we first define $\beta_J^T := [\beta_0, \dots, \beta_{JL}]^T = h(n) \star_J h(n)$ the J -fold convolution of $h(n)$ with itself that we denote as \star_J . It then follows that: $H^J(\rho_m) := H^J(z)|_{z=\rho_m} := (\beta_0 + \dots + \beta_{JL}z^{-JL})|_{z=\rho_m}$. To determine the coefficients $\beta_0, \dots, \beta_{JL}$ uniquely from $H^J(\rho_m)$, we need $JL + 1$ distinct such equations that become available when ρ_m takes $JL + 1$ distinct values. Therefore, selecting block length $M \geq JL + 1$ allows one to find $\beta_0, \dots, \beta_{JL}$ uniquely, which enables determination of $H^J(z) = \sum_{i=0}^{JL} \beta_i z^{-i}$ on the entire complex plane. Observing that $H^J(z)$ is formed by all the roots of $H(z)$ with multiplicity J , we can extract from the roots of $H^J(z)$ those L roots that form $H(z)$. This implies that $H(z)$ is uniquely identifiable up to a scalar ambiguity, as we summarize in the following proposition:

Proposition 1: *If the length of a symbol block M (which is a system design parameter) satisfies $M \geq JL + 1$, identifiability of the L th-order channel $H(z)$ is guaranteed from the demodulated data $y(i; m) = H(\rho_m)s(i; m)$ under assumptions a1a) and a1b) with J specified as in Definition 1.*

With channel nulls on subcarriers, symbols are not recoverable as one can verify from (8). Although equalizability is not assured, blind channel identifiability is established here by Proposition 1 regardless of channel zero locations, unlike the subspace based method derived in [5] for CP-OFDM.

Under a2), we have $E\{\tilde{\eta}^n(i; m)\} = 0 \forall n > 0$, regardless of the noise color. Note also that $\tilde{\eta}(i; m)$ is complex circular Gaussian even with BPSK because it models noise after FFT processing. With J as in Definition 1, a2) implies that $E\{y^J(i; m)\} = E\{[H(\rho_m)s(i; m) + \tilde{\eta}(i; m)]^J\} = H^J(\rho_m)E\{s^J(i; m)\}$, and hence (9) still holds true. In practice, $E\{y^J(i; m)\}$ is replaced by consistent sample averages (over I blocks), and thus $H^J(\rho_m)$ is estimated as:

$$\hat{H}^J(\rho_m) = \frac{-Q}{J\alpha_J} \left(\frac{1}{I} \sum_{i=0}^{I-1} y^J(i; m) \right), \quad m \in [0, M-1]. \quad (10)$$

We next collect $\hat{H}^J(\rho_m)$ from (10) in an $M \times 1$ vector: $\hat{\mathbf{h}}_J := [\hat{H}^J(\rho_0), \dots, \hat{H}^J(\rho_{M-1})]^T$, and define matrix $\mathbf{V}_J := [\mathbf{v}_{JL+1}(\rho_0), \dots, \mathbf{v}_{JL+1}(\rho_{M-1})]^T$, where $\mathbf{v}_D(\rho) := [1, \rho^{-1}, \dots, \rho^{-D+1}]^T$ is a $D \times 1$ Vandermonde vector formed by the constant ρ . With $\hat{\mathbf{h}}_J = \mathbf{V}_J \hat{\beta}_J$ describing the \mathcal{Z} -transform of $\hat{\beta}_J$ evaluated at $\{z = \rho_m\}_{m=0}^{M-1}$, $\hat{\beta}_J$ can then be estimated by a simple inversion (\dagger denotes matrix pseudo-inverse) as:

$$\hat{\beta}_J = \mathbf{V}_J^\dagger \hat{\mathbf{h}}_J. \quad (11)$$

Relying on the FFT-processed data $y(i; m)$ in (8) and capitalizing on the finite alphabet of $s(i; m)$, (10) and (11) provide sufficient information to recover \mathbf{h} . Starting from time domain vector (11) only, and based on the fact that β_J has all L roots of \mathbf{h} with multiplicity J , we can search over JL noisy roots of $\hat{\beta}_J$ and find that combination of L roots that matches \mathbf{h} best. (this corresponds to the Root Selection (RS) algorithm in [8]). However, complexity of the RS increases fast as J, L increase and this nonlinear algorithm will exhibit sensitivity when roots are to be found in the presence of noise. It is possible however, to derive a Linear Equations (LE) based channel estimator by observing that $\hat{\beta}_J$ is the J -fold linear convolution of \mathbf{h} [8]. Although very simple to implement, the LE method is prone to noise-induced error propagation when $|h(0)|$, or $|h(L)|$, is small. Therefore, the LE method is only well motivated for wired-line applications where the strong path is synchronized as the first

path. We next will describe channel estimators starting from the frequency domain estimates in (10).

A. MINIMUM-DISTANCE ALGORITHMS

Given $\hat{H}^J(\rho_m)$ estimates from (10), we develop here two Minimum Distance (MD) approaches. For each $m \in [0, M-1]$, we have $\hat{H}^J(\rho_m) = \lambda_m [\hat{H}^J(\rho_m)]^{1/J}$, where $\lambda_m \in \{\exp(j2\pi n/J)\}_{n=0}^{J-1}$ is the corresponding scalar ambiguity in taking the J th root, $\forall m$. To resolve these ambiguities, we exhaustively search over all J^M possible vectors $\hat{\mathbf{h}}_1 := [\lambda_0 [\hat{H}^J(\rho_0)]^{1/J}, \dots, \lambda_{M-1} [\hat{H}^J(\rho_{M-1})]^{1/J}]^T$. For each $\hat{\mathbf{h}}_1$, we compute the corresponding time domain vector through Least Squares fitting: $\hat{\mathbf{h}}_1 = \mathbf{V}_1^\dagger \hat{\mathbf{h}}_1$, where $\mathbf{V}_1 := [\mathbf{v}_{L+1}(\rho_0), \dots, \mathbf{v}_{L+1}(\rho_{M-1})]^T$ is the Vandermonde matrix that relates channel frequency responses with time domain channel coefficients. Channel estimates are then found by minimizing the Euclidean distance:

$$\hat{\mathbf{h}} = \arg \min_{\hat{\mathbf{h}}_1} \|\hat{\beta}_J - \hat{\mathbf{h}}_1 \star_J \hat{\mathbf{h}}_1\|. \quad (12)$$

Instead of (12), a joint maximum likelihood (ML) channel and symbol estimation could be pursued based on the noisy data in (8), by searching for the best fit over all possible symbol and channel combinations. Because both ML and MD resort to exhaustive search, it is of interest to compare them. If we collect I blocks (each of length M), the complexity of ML for a Q -ary constellation is proportional to Q^{JM} while the complexity of MD reduces to only J^M by exploiting the known signal constellation to eliminate the unknown symbols $s(i; m)$. MD and ML have the same complexity when the ML operates on a single block and the constellation has size $J = Q$. In this case however, the MD will perform significantly better than ML because it decreases additive noise through block averaging (c.f. (10)) rather than operating on the scalar noisy samples of (8). Although less complex than ML, the MD approach is still too complex to be implemented because often $M \gg L$ in practical systems. However, it is always useful as a bound to benchmark performance of simpler channel estimators.

Because the channel order $L < M$, the MD method does not require the entire vector $\hat{\mathbf{h}}_1$ to obtain the time-domain channel estimate $\hat{\mathbf{h}}_1$. This observation motivates the following modified Minimum Distance (MMD) algorithm:

- 1) select \bar{N} elements from $\hat{\mathbf{h}}_1$ and form a new $\bar{N} \times 1$ vector $\tilde{\tilde{\mathbf{h}}}$. For $J^{\bar{N}}$ possible $\tilde{\tilde{\mathbf{h}}}$, we obtain the time domain $\hat{\mathbf{h}}_1 = \tilde{\mathbf{V}}^\dagger \tilde{\tilde{\mathbf{h}}}$, where $\tilde{\mathbf{V}}$ is constructed from \mathbf{V}_1 by keeping only the corresponding \bar{N} rows. The only requirement on \bar{N} is to satisfy $\bar{N} \geq L+1$, such that $\tilde{\mathbf{V}}^\dagger$ exists. We can choose those \bar{N} elements with largest absolute values, or simply focus on \bar{N} equispaced subcarriers.
- 2) obtain channel estimates as in (12).

The complexity is now reduced from J^M to $J^{\bar{N}} \geq J^{L+1}$, rendering the MMD algorithm affordable for low order channels. Presence of (say N_p) pilot tones will reduce the complexity of MMD further. Indeed, as we will describe later on, we can determine the phases λ_m on those pilot carriers (c.f. (13)). Including those frequency responses in $\tilde{\tilde{\mathbf{h}}}$, we only need to search over $J^{\bar{N}-N_p}$ possible choices. The complexity is then $1/J^{N_p}$ of that without pilot tones, which makes the MMD applicable to longer channels with the same complexity.

B. PHASE AMBIGUITY RESOLVING ALGORITHM

As described in the MD approach, for each m we obtain $\hat{H}^J(\rho_m) = \lambda_m [\hat{H}^J(\rho_m)]^{1/J}$ up to a scalar ambiguity constant

$\lambda_m \in \{\exp(j2\pi n/J)\}_{n=0}^{J-1}$. Suppose that initial estimates $\hat{H}_0(\rho_m)$ are available. For each $m \in [0, M-1]$, we can resolve the phase ambiguity by searching over J candidate phase values:

$$\hat{\lambda}_m = \arg \min_{\lambda_m} |\hat{H}_0(\rho_m) - \lambda_m [\hat{H}^J(\rho_m)]^{1/J}|^2. \quad (13)$$

Therefore, we can improve channel estimation accuracy through the Phase Ambiguity Resolving (PHAR) steps that we describe next:

S1) set $i_1 = 0$, find an initial estimate $\hat{\mathbf{h}}_0$ using low complexity methods, and calculate the frequency response $\hat{H}_0(\rho_m)$ for $m = 0, 1, \dots, M-1$.

S2) in each successive iteration, set $i_1 := i_1 + 1$, and

a) resolve phase ambiguities by replacing $\hat{H}_0(\rho_m)$ with $\hat{H}_{i_1-1}(\rho_m)$ in (13) and form the vector $\hat{\mathbf{h}}_1 := [\hat{\lambda}_0 [\hat{H}^J(\rho_0)]^{1/J}, \dots, \hat{\lambda}_{M-1} [\hat{H}^J(\rho_{M-1})]^{1/J}]^T$;

b) update channel estimates $\hat{\mathbf{h}}_{i_1} = \mathbf{V}_1^\dagger \hat{\mathbf{h}}_1$, and their frequency response using $\hat{\mathbf{h}}_{i_1} = \mathbf{V}_1 \hat{\mathbf{h}}_{i_1}$.

S3) repeat S2 several (say I_1) times, or, continue until $\hat{\mathbf{h}}_{i_1} \approx \hat{\mathbf{h}}_{i_1-1}$ in the Euclidean norm sense.

It is worth recalling that $J = 2$ for BPSK and hence $\lambda_m \in \{\pm 1\}$. For the widely used QPSK, 16QAM and 64QAM we have $J = 4$ so that $\lambda_m \in \{\pm 1, \pm j\}$. These few phase values can be resolved easily via (13) with high accuracy even when coarse initial channel estimates are only available.

An alternative means of capitalizing on the finite-alphabet is the Decision-Directed (DD) algorithm (see e.g., [8]), which performs symbol estimation first based on initial channel estimates and then estimates the channel by treating the symbol estimates as known symbols. Serving a similar purpose, the PHAR algorithm outperforms the DD iteration for two reasons:

- i) The DD algorithm diverges easily at low SNR because symbol by symbol detection has poor performance. The smallest Bit Error Rate (BER) will be that corresponding to known channels. In contrast, the PHAR algorithm can reduce noise effects (and thus channel estimation error) to arbitrarily low levels by collecting more and more blocks. Therefore, channel estimation accuracy can be improved consistently;
- ii) DD performance degrades as the constellation size increases because the minimum Euclidean distance among constellation points decreases. In the PHAR algorithm however, $J = 4$ for all QAM signals and the same number of possible phase values $\{\pm 1, \pm j\}$ is present regardless of the constellation size.

The price paid by PHAR is a certain amount of “mismatch noise” that arises due to finite sample effects when ensemble quantities in (9) are replaced by sample averages in (10). This mismatch is not present with PSK signals because $s^J(i; m) = -1$ (or 1 for BPSK) deterministically; i.e., ensemble averages coincide with sample averages. In noise-free reception, the DD algorithm converges to the ML solution and perfect channel estimates are obtained. PHAR on the other hand, will be affected by the finite sample size for signals other than PSK and its channel estimation error curves will level-off (floor effect). However, the error floor can be lowered to a prescribed level by collecting a sufficient number of blocks. Alternatively, it is even possible to eliminate the error floor by applying the DD iteration only once. This remedy though is only effective at high SNR values for large signal constellations, as will be illustrated in our simulations.

In addition to having low complexity and high channel estimation accuracy, the PHAR algorithm lends itself naturally to tracking. Among many window choices, we can form sliding window (of size W) channel estimates by averaging only the W most recently received blocks $\{\mathbf{y}(i)\}_{i=L-W+1}^L$ in (10) to obtain:

$$\hat{H}_{i+1}^J(\rho_m) = \hat{H}_i^J(\rho_m) + \frac{-Q}{J\alpha_J} [y^J(i+1; m) - y^J(i-W+1; m)]. \quad (14)$$

We then can apply the PHAR algorithm to the new estimates $\{\hat{H}_{i+1}^J(\rho_m)\}_{m=0}^{M-1}$ and use the current $\hat{H}_i^J(\rho_m)$ as an initial estimate $\hat{H}_0(\rho_m)$ in (13). Combining channel estimates in (14) with the phase resolving step of (13) equips PHAR with a low complexity tracking capability.

Because training sequences are provided in practical systems, we can initialize our PHAR algorithm either for improving channel estimation accuracy or for tracking channel variations with training based channel estimates. Such a semi-blind channel estimation method has only linear complexity and is thus very simple when compared to the cubic complexity of matrix SVD decompositions required by subspace based methods.

PHAR advantages over DD have practical ramifications. In a nutshell: either starting from low complexity blind channel estimators, or, by exploiting training sequences present in current OFDM standards, the PHAR algorithm yields the best achievable MD performance with reduced complexity and is capable of tracking slow channel variations.

C. DISTINCT FEATURES

We present next some unique characteristics of our channel estimation methods.

C.1. NOISE EFFECTS AND CONVERGENCE ISSUES

To appreciate how our blind channel estimators handle noise effects, it is of interest to compare them with benchmark methods that are based on training. For one training block $\{s(i; m)\}_{m=0}^{M-1}$, we receive $y(i; m) = H(\rho_m)s(i; m) + \tilde{\eta}(i; m)$. The effective signal to noise ratio (SNR) for channel estimation is thus $|H(\rho_m)|^2 \sigma_s^2 / \sigma_{\tilde{\eta}}^2$, where σ_s^2 ($\sigma_{\tilde{\eta}}^2$) stands for signal (noise) power. Our blind methods will first take the J th power of the received FFT-processed data to obtain:

$$y^J(i; m) = H^J(\rho_m)s^J(i; m) + J\tilde{\eta}(i; m)s(i; m)H(\rho_m) + O(\tilde{\eta}^2(i; m)).$$

The SNR pertinent to channel estimation is now $|H(\rho_m)|^2 \sigma_s^2 / (J^2 \sigma_{\tilde{\eta}}^2)$, showing $10 \log(J^2)$ dB (6dB for BPSK) loss relative to the training based method. However, this noise enhancement can be remedied by averaging across many (say I) blocks as per (10), which increases the SNR by $10 \log_{10} I$ (dB). Therefore, our method based on $I = 4$ BPSK OFDM symbols (or $I = 16$ for QPSK, 16QAM and 64QAM) approximates the channel estimation accuracy reachable by one training block. As additional blocks become available, channel estimation accuracy improves and our blind method outperforms the bandwidth-consuming training based method.

In addition to alleviating noise effects, block averaging in (10) approximates ensemble quantities by sample averaging. For constellations other than PSK, we need to collect sufficient number of blocks to decrease such finite sample effects that are prevalent especially at high SNR where additive noise can be omitted. Recall however, that $s^J(i; m)$ assumes a small number of values e.g., 4 distinct values for 16QAM and 16 distinct values for 64QAM signaling. This alleviates the requirement

on the number of blocks I . For PSK transmissions, our channel estimators do not rely on statistical properties of $s(i; m)$ as required by assumption a1b) since $s^J(i; m) = -1$ (or 1 for BPSK) deterministically. Even one block is then sufficient to yield reliable channel estimates at high SNR with guaranteed channel identifiability.

C.2. SCALAR AMBIGUITY DETERMINATION

All blind estimators of a channel \mathbf{h} come with an inherent (generally complex) scalar ambiguity, namely blind channel estimates $\hat{\mathbf{h}}$ satisfy $\mathbf{h} = \alpha \hat{\mathbf{h}}$, where $\alpha \in \mathbb{C}$. In practice, a few pilot tones are used to determine α by comparing the estimated with the known frequency response on those pilot carriers. Because both channel estimates as well as pilot tones are contaminated by noise, such a matching may not be accurate. It can even be misleading if the channel responses on those pilot carriers are not estimated accurately. However, because $H^J(z) = \alpha^J \hat{H}^J(z)$ in our approach, the scalar ambiguity reduces from infinite choices to the finite set $\{\exp(j2\pi n/J)\}_{n=0}^{J-1}$. As $J = 2$ or 4 for most practical signal constellations, the set is simply $\{\pm 1\}$ or $\{\pm 1, \pm j\}$. Thus, the task of recovering α is simplified considerably. Only one pilot symbol suffices to resolve this phase ambiguity by picking the correct phase from a few choices.

Note that our simplified scalar determination can also be utilized by other blind channel estimation methods. For example, the subspace methods of [5] and [6] can estimate the channel as $\hat{\mathbf{h}}_s$ first, based on structure information. They can then exploit the finite alphabet property of the symbols and reduce the scalar ambiguity α to J finite values by matching $\alpha^J \hat{\mathbf{h}}_s \star_j \hat{\mathbf{h}}_s$ with β_j . Therefore, simply by reducing the scalar ambiguity to a finite phase values first, one can resolve the phase ambiguity accurately using a few pilots even for other blind channel estimation methods [5],[6].

IV. COMPARISONS AND SIMULATED PERFORMANCE

In this section, we will illustrate the merits of our blind channel estimators through simulations. The figure of merit here is the normalized least-squares channel error (NLSCE) defined in the frequency domain as: $\sum_{m=0}^{M-1} [H(\rho_m) - \hat{H}(\rho_m)]^2 / \sum_{m=0}^{M-1} [H(\rho_m)]^2$.

Test case 1: We set $M = 16$, $L = 1$ (two-ray channels), $I = 200$, and average over 500 randomly generated channels each with independent Rayleigh distributed taps. We test four widely used signal constellations: BPSK, QPSK, 16QAM, 64QAM. However, due to space limitations and the similar behavior exhibited by BPSK and QPSK, 16QAM and 64QAM, we will only show representative results for BPSK and 64QAM. To allow for a fair comparison among different signal constellations, we normalize signal power to the same bit energy E_b . To benchmark our blind channel estimation methods, we also examined a standard training (TR) based method that relies on two known symbol blocks:

We present in Figs. 3 and 4 the TR, MD, MMD channel estimators (with $\bar{N} = L+1$ equispaced subcarriers) as well as the MMD followed by several PHAR or DD iterations; First, we see that MD benchmarks all other blind channel estimators and outperforms the TR method. The MMD offers rather good channel estimates, it outperforms the TR with BPSK and it is comparable to TR with 64QAM. Few PHAR ($I_1 = 2$) refinements suffice to make the MMD algorithms approach the best achievable MD performance. At low SNR, DD diverges due to a poor symbol estimation step. However, PHAR improves

significantly by averaging across blocks. Error floor appears when our method is applied to large signal constellations at high SNR. However, the error floor can be lowered by collecting more blocks. In Figs. 5 and 6, we initialize PHAR and DD with channel estimates obtained from training. We see that the floor level decreases as the number of blocks increases in Fig. 6. We can eliminate this error floor by applying one DD iteration to TR-PHAR (denoted by TR-PHAR-DD). In Fig. 6, we see that TR-PHAR-DD outperforms TR-PHAR for $E_b/N_0 > 7$ dB. However, it diverges at low SNR due to the limited symbol estimation accuracy. There is no error floor for PSK transmissions and as we deduce from Fig. 5, TR-PHAR is always better than TR-PHAR-DD. Therefore, applying one DD iteration is only effective at high SNR and for large signal constellations. However, in such cases we see from Fig. 6 that PHAR offers accurate enough channel estimates.

Test case 2: Here we test application of the PHAR algorithm to the HIPERLAN/2 system [7] where OFDM transmission is utilized with $M = 64$ subcarriers (frequency spacing $312.5kHz$) and a CP of length $L = P - M = 16$. Note that $M < 4L + 1$ which according to Proposition 1 implies that blind channel identifiability holds for BPSK, but not for QPSK and 16 or 64QAM signaling with $J = 4$. However, we can apply the PHAR algorithm directly to the standard with training based initialization, because the identifiability requirement is now reduced to $M \geq L + 1$ thanks to known training symbols.

We compare performance of the classical training based method against our semi-blind TR-PHAR method using the channel model A in [2] with truncated $L+1 = 17$ taps that are Rayleigh distributed. For space limitations, we only present the result for slowly time-varying channels with Jakes's Doppler spectrum at $v = 10$ m/s and a typical SNR of $E_b/N_0 = 10$ dB with a sliding window of size $W = 100$ in (14). Fig. 7 verifies that TR-PHAR tracks closely, while TR is unable to track slow channel variations. TR-PHAR's excellent tracking capability supports its potential in mobile communications.

V. CONCLUSIONS

A new finite-alphabet based channel estimation approach has been developed in this paper and shown to possess attractive features not only for the classical CP-OFDM but also for the modified TZ-OFDM. Being simple and flexible it holds high application potential for existing OFDM standards and future generation multicarrier systems. Those include also wide-band CDMA hybrids that rely on multicarrier transmissions to suppress multi-user interference and reduce channel estimation to the OFDM-like single-user problem treated in this paper. The channel estimation algorithms derived herein offer choices to trade off performance with complexity, while guaranteeing channel identifiability regardless of channel zero locations. They reduce estimation of the scalar ambiguity inherent to all blind channel estimators to a small number of phase values. Especially with PSK modulated signals, high estimation accuracy is achieved with minimal received data. By exploiting training data usually specified in OFDM standards, semi-blind and adaptive implementations were shown to improve estimation accuracy and be capable of tracking channel variations with surprisingly low complexity.

REFERENCES

- [1] J. A. C. Bingham, "Multicarrier modulation for data transmission: An idea whose time has come," *IEEE Communications Magazine*, pp. 5-14, May 1990.

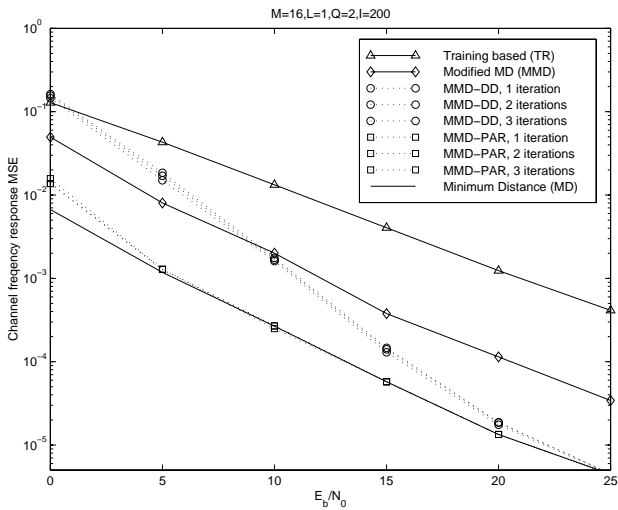


Figure 3: Comparisons of channel estimators (BPSK)

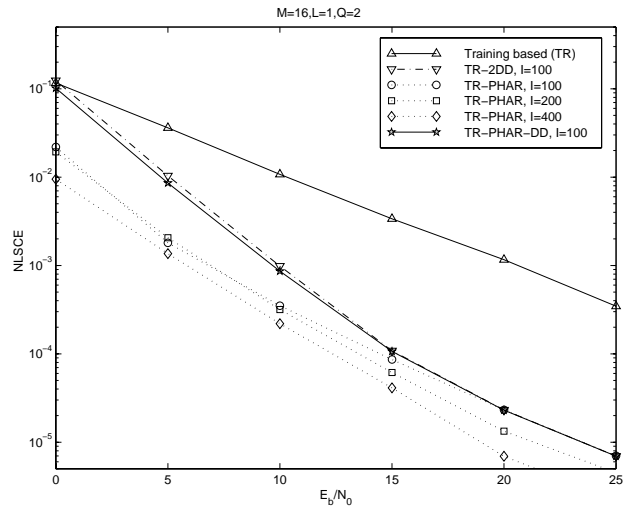


Figure 5: Error floor effects (BPSK)

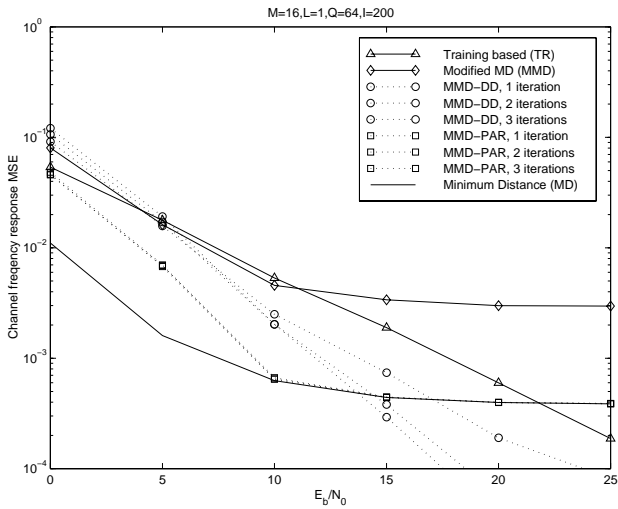


Figure 4: Comparisons of channel estimators (64QAM)

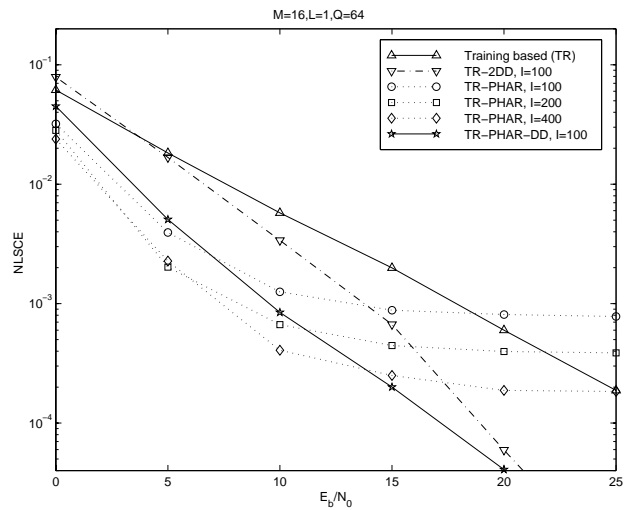


Figure 6: Error floor effects (64QAM)

- [2] ETSI Normalization Committee, "Channel models for HIPERLAN/2 in different indoor scenarios," Norme ETSI, document 3ER1085B, European Telecommunications Standards Institute, Sophia-Antipolis, Valbonne, France, 1998.
- [3] G. H. Golub and C. F. Van Loan, *Matrix Computations*, Johns Hopkins University Press, 3rd edition, 1996.
- [4] R. W. Heath and G. B. Giannakis, "Exploiting input cyclostationarity for blind channel identification in OFDM systems," *IEEE Trans. on Signal Processing*, vol. 47, pp. 848–856, 1999.
- [5] B. Muquet, M. de Courville, P. Duhamel, and V. Buénac, "A subspace based blind and semi-blind channel identification method for OFDM systems," in *Proc. of IEEE-SP Workshop on Signal Proc. Advances in Wireless Comm.*, Annapolis, MD, May 9-12, 1999, pp. 170–173.
- [6] A. Scaglione, G. B. Giannakis, and S. Barbarossa, "Redundant filterbank precoders and equalizers Part II: Blind channel estimation, synchronization, and direct estimation," *IEEE Transactions on Signal Processing*, vol. 47, pp. 2007–2022, July 1999.
- [7] R. D. J. van Nee, G. A. Awater, M. Morikura, Hi. Takanashi, M. A. Webster, and K. W. Halford, "New high-rate wireless LAN standards," *IEEE Comm. Magazine*, vol. 37, Dec. 1999.
- [8] S. Zhou, G. B. Giannakis, and A. Scaglione, "Long codes for generalized FH-OFDMA through unknown multipath channels," *IEEE Transactions on Communications*, submitted Oct. 1999; see also <http://www-mount.ee.umn.edu/~gg3/shengli/gfh.ps>

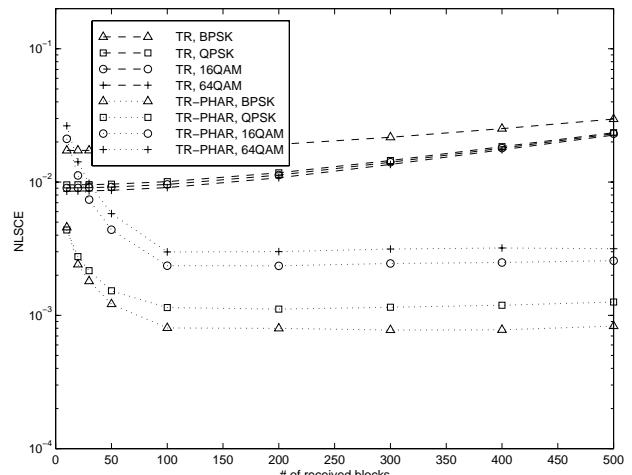


Figure 7: Application to the HIPERLAN/2 system